Enhanced Light Confinement in a Near-Field Optical Probe with a Triangular Aperture

A. Naber,* D. Molenda, U. C. Fischer, H.-J. Maas, C. Höppener, N. Lu, and H. Fuchs

Physics Institute, Wilhelm-Klemm-Strasse 10, D-48149 Münster, Germany

(Received 15 March 2002; published 31 October 2002)

We present a probe concept for scanning near-field optical microscopy combining the excellent background suppression of aperture probes with the superior light confinement of apertureless probes. A triangular aperture at the tip of a tetrahedral waveguide (full taper angle $\sim 90°$) shows a strong field enhancement at only one rim when illuminated with light of suitable polarization. Compared to a circular aperture of equivalent size, the resolution capability is doubled without loss of brightness. For a ~ 60 nm sized triangular aperture, we measured an optical resolution < 40 nm and a transmission of $\sim 10^{-4}$.

DOI: 10.1103/PhysRevLett.89.210801 PACS numbers: 07.79.Fc, 42.25.Gy, 78.55.–m, 78.67.–n

In contrast to conventional light microscopy, scanning near-field optical microscopy (SNOM) is able to achieve an optical resolution well below the classical diffraction limit of about half the wavelength of light [1–3]. The heart of this method is a submicroscopic light source, which probes a surface point by point at a distance of only a few nanometers. The optical resolution of SNOM is independent of the wavelength of propagating light, but scales with the size of the light source and its distance from the investigated surface. The intensity of light radiating from an optical probe into the far field decreases strongly with decreasing size of the source. Therefore, the challenge in designing an optical probe for SNOM lies in the need for the realization of two contrary demands: A sufficient brightness of the light source and, simultaneously, a confinement of light to dimensions far below the wavelength.

Since the invention of SNOM many different concepts for the realization of near-field optical probes have been proposed [3]. These concepts are generally divided into two groups, so-called aperture probes and apertureless probes. The key element of an apertureless probe is a submicroscopic metallic particle, e.g., a protrusion in a metal film [4], a metal grain at the end of a waveguide [5,6] or a sharp metallic tip [7–11], which produces a high local electric field enhancement when it is illuminated with light. Several groups reported optical superresolutions in the range of 1–10 nm [6,8]. In the case of aperture probes [12], the light emerges from an aperture in an otherwise opaque metallic film. For the most common type of aperture probe, a metal coated tapered optical glass fiber is used as a waveguide directing light to the aperture at the pointed end [2,13,14]. The penetration depth of light into the metallic coating sets a lower limit of ~ 12 nm for the optical resolution [2]. Most applications, however, require a much higher light intensity than common fiber probes with small apertures can provide, so that aperture diameters of 80–100 nm are actual practice [12]. A benefit of aperture probes is the low level of nonlocal background light, which makes it easier to achieve a sufficient signal-to-noise ratio and reduces the probability for the destruction of photo-labile dye molecules in fluorescence applications.

Despite the apparently different underlying physical principles of SNOM probes with and without aperture, a fundamental relationship between both approaches was revealed by near-field optical fluorescence measurements of single molecules [15–17]. A high local field enhancement at the rims of a circular aperture governed the measured fluorescence pattern, if the imaged molecules were partially oriented vertically. Just as for apertureless probes, the strong field enhancement was caused by light induced surface charges at the metallic edges. Because of the symmetry of a circular aperture, however, it was inevitable that the strongly localized electric field appeared with equal intensity at least at two opposing edges, so that one molecule generally gave rise to at least two fluorescence spots. Therefore, a substantial increase of optical resolution would result if it were possible to enhance the field at one edge clearly more than at the others. Apparently, this can be accomplished only by reducing the symmetry of the aperture.

We show in this Letter that a triangular aperture (TA) at the tip of a tetrahedral hollow waveguide exhibits a clearly predominant field enhancement at only one of its three edges when illuminated with light of suitable polarization. Compared to a circular aperture of equivalent size, the optical resolution capability is approximately doubled without a corresponding loss of brightness. Thus, a TA probe may be considered as a unique combination of an aperture probe with its excellent suppression of background light and an apertureless probe with its superior confinement of light. It is demonstrated that a TA probe is particularly suited to fluorescence measurements in a resolution range clearly < 40 nm.

So far, a triangular aperture has been investigated neither experimentally nor theoretically in the context of near-field optical microscopy. By applying a recently introduced characterization method for SNOM probes [18] to the TA probe, we are able to determine the

topography and the electric field distribution within the TA and in its immediate vicinity. This method is based on simultaneous force and near-field optical imaging of (20 ± 4) nm sized polystyrene spheres doped with fluorescing dye molecules. Because of the small size of such a nanosphere as compared to the aperture, probe and sample are reversing their roles during the imaging process. Thus, the measured topography is an image of the end face of the probe, and the optical image displays the distribution of the electric field intensity at the aperture.

We have developed a simple method, which allows us to fabricate routinely TA probes with a small aperture size and a full taper angle of $\sim 90°$. A small piece of glass is broken out of a cover slide in such a way that three orthogonal edges are leading to a common ultrasharp corner [6]. After rotational evaporation of ~ 100 nm aluminum, the probe is attached to a piezoelectric quartz tuning which is used as a force sensor for tip-sample distance control [Fig. 1(a)] [19]. A tiny prism at the rear of the probe enables us to irradiate a tightly focused light beam into the tip along the axis of symmetry which is oriented normal to the surface [Fig. 1(b)]. After approaching the probe to an uncovered region of a nanosphere sample, an aperture at the very end of the coated tip is created by controlled squeezing against the flat glass surface [1,14]. From the geometry of the glass tip, the aperture may be expected to have a shape of an equilateral triangle.

At first, we will show results of a TA probe which has been heavily squeezed to get a large aperture. Figure 2(a) displays a scanning electron microscope (SEM) image of the end face of a probe exhibiting an aperture with the shape of an equilateral triangle and a side length of ~ 130 nm. The topographic image in Fig. 2(b), which has been measured by means of a ~ 24 nm sized nanosphere, reveals a tetrahedron-shaped protrusion at the location of the aperture. This protrusion very likely represents the tip of the uncovered glass body, which squeezed through the aluminum and then penetrated into the sample surface while the metal film was kept back. Owing to the hard surface contact, the initially ultrasharp glass tip was considerably rounded off, so that the foremost tip lost the tetrahedral shape. The flat end face beyond the aperture is not detected by the nanosphere because its diameter is smaller than the protrusion. Simultaneously to the topography, several fluorescence images have been taken for different polarization directions of the illuminating light [Figs. 2(c)–2(f)]. The accompanying topographic images, which are similar to Fig. 2(b), have been used to compensate for the lateral drift, so that every optical image displays exactly the same part of the end face. An equilateral triangle has been inserted in the images to identify the rim of the aperture as it is concluded from the SEM image and the topography. For the fluorescence measurement in Fig. 2(c), the polarization was adjusted parallel to the left triangle side (edge 1). As a result, two spots of almost similar brightness appear which are aligned along the direction of polarization and whose maxima are separated from each other by ~ 110 nm. Such a field distribution pattern is well known from theoretical [20,21] as well as experimental investigations [13,15,16] of circular apertures illuminated with linearly polarized light. There, the light-electric field irradiated into the aperture is partly compensated by a depolarization field generated by opposite surface charges at the metallic rim [21]. These surface charges are responsible for the strong field enhancement. We assume the origin of the spots in Fig. 2(c) to be caused by the same effect, and we identify the location of the spots with edges 2 and 3, respectively, of the triangular aperture. This interpretation is strongly supported by the differing orientations of the elliptic fluorescence spots. For the measurement in Fig. 2(d), the polarization was rotated by 90°, so that the electric field vector was perpendicular to edge 1. Surprisingly, in

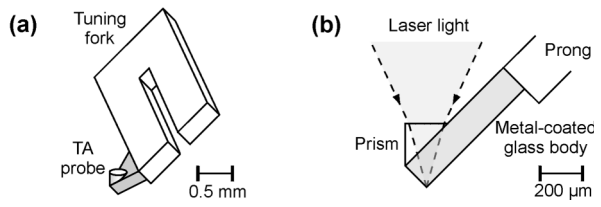

FIG. 1. (a) Schematic of a TA probe attached to a tuning fork as a force sensor for feedback control. Probe and tuning fork are tilted such that the symmetry axis of the probe is oriented normal to the surface. (b) Enlarged side view. A tiny prism on the rear of the glass body enables the illumination of the aperture with focused laser light.

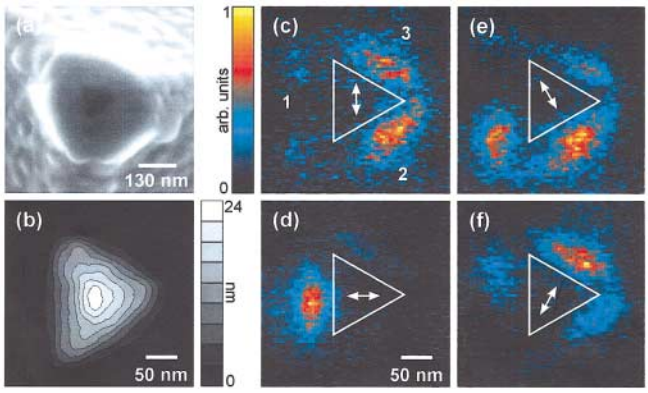

FIG. 2 (color). Characterization of a TA probe with a large aperture. (a) The SEM image shows an equilateral triangular aperture (side length ~ 130 nm), whereas (b) the topography reveals a tetrahedron-shaped protrusion at the location of the aperture. (c)–(f) The simultaneously taken fluorescence images display the intensity distributions of the electric field for several different directions of the irradiated linearly polarized light (see arrows). A white triangle marks the rim of the aperture as concluded from (a) and (b).

this situation only one single spot along edge 1 is produced. Obviously, only edge 1 of the aperture exhibits a strongly enhanced electric field, whereas at the other two edges almost no enhancement arises. To our knowledge, such a phenomenon has not been reported before in the field of near-field optics. Because of the suppression of a second spot, the optical resolution capability is considerably improved though the total intensity practically is not affected. The full width at half maximum (FWHM) of the elliptic fluorescence spot is ~80 nm along the long axis and ~40 nm along the short axis. Owing to the symmetry of the probe, a similar confinement effect should occur when the polarization direction is rotated by −60° or 60°. As can be seen from Figs. 2(e) and 2(f), this is really the case, however, the electric field intensity at the nonperpendicular edges is no longer fully suppressed. Very likely, this result is due to a break of the threefold symmetry in the experimental arrangement. We tentatively attribute the observed asymmetry to a deviation of the direction of the incident light beam from the principal axis of the probe. Experimental evidence for this hypothesis, however, is not easy to produce since at the moment the geometry and orientation of the tip cannot be strictly controlled in the fabrication process. As an alternative approach we are currently investigating the field distribution by a numerical simulation. These calculations, however, are rather complex since the properties of the tetrahedral waveguide probably have a strong influence on the field distribution. Therefore, a simulation cannot be restricted to only the very end of the probe.

Though it is evident that the measured effects are connected to an equilateral triangular aperture, the measured fluorescence spots seem to be rather far away from the rims of the aperture (~ 50 nm). This can be partly understood by taking into account the wide taper angle of the glass body. The thickness of the metal film at the flattened end face increases only gradually with increasing distance to the aperture, so that the film close to the rim is not fully opaque. Therefore, the effective optical aperture may be larger than the aperture measured with the SEM. A further shift of the fluorescence spots relative to the rim of 20–25 nm can be attributed to a rapid decrease of optical resolution with increasing effective probe-sample distance as it was recently observed for single molecule imaging with circular apertures [16,17]. If we take both effects into account, an effective optical aperture with a side length of ~160 nm is in good agreement with our experimental findings. By comparing this length with the measured extension of the electric field at the rim, we conclude, that the optical resolution capability of a TA probe scales with about half the side length of the effective optical aperture.

We are also able to create very small apertures by the squeezing method. Figure 3(a) shows a SEM micrograph of a TA probe with an apparent aperture size of ~35 nm (FWHM). Again, the topographical image [Fig. 3(b)] exhibits a protrusion at the lateral position of the aperture. As in Fig. 2(b), the tip of the protrusion is markedly rounded off, which readily explains why the shape of the SEM aperture appears to be not triangular. However, the result of the optical characterization [Figs. 3(c) and 3(d)] strongly suggests that the effective optical aperture is again an equilateral triangle, here with a side length of ~60 nm. Since the resolution capability in case of the large aperture scaled with half the triangle side length, the best possible optical resolution for this probe is assumed to be ~30 nm for closest proximity to the sample. The extension of the single fluorescence spot in Fig. 3(d), however, is considerably larger. We think this result is due to a no more negligible size of the imaged nanosphere as compared to the resolution capability of the probe.

In order to demonstrate that the optical resolution can indeed approach a value close to 30 nm, we present topographical and near-field optical fluorescence images of aggregates of only ~5 nm sized CdSe nanocrystal quantum dots (QDs) [22] (Fig. 4). The polarization of the incident laser light was adjusted as shown in Fig. 3(d). The QD aggregates self-assembled over an area of several mm^2 in almost linear chains of ~1 μm distance by means of a recently introduced template of equally spaced channel structures in a ~2 nm thick Langmuir-Blodgett (LB) film [23]. By force distance control, a clear image of the topography of channels and aggregates was obtained [Fig. 4(a)]. The simultaneously taken SNOM image [Fig. 4(b)] proves that the small particles in Fig. 4(a) are indeed aggregated or single QDs since they are strongly fluorescing. Even very closely neighbored aggregates (< 100 nm) can be easily distinguished in the optical image, and for the smallest aggregates, the FWHM of the fluorescence spots

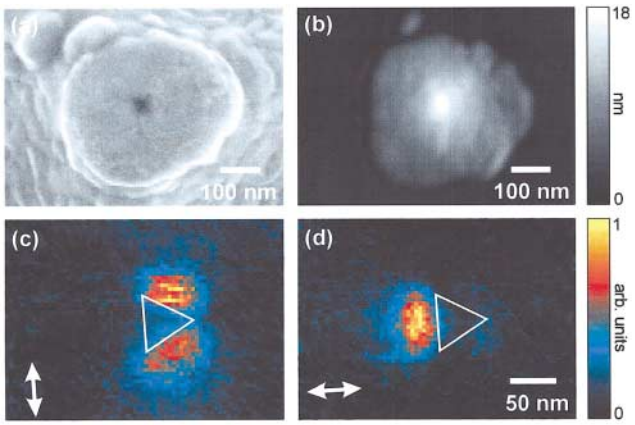

FIG. 3 (color). Characterization of a TA probe with a small aperture. (a) SEM image: aperture size is ~35 nm (FWHM). (b) Topography: A small rounded tip at the location of the aperture protrudes from an otherwise flat end face. (c),(d) Optical field distributions at the aperture for two different polarization directions of the incoming light (see arrows). A white triangle marks the rim of the effective optical aperture.

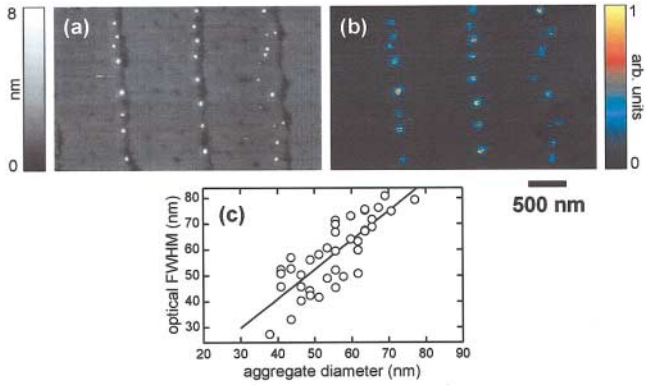

FIG. 4 (color). (a) Topographic and (b) fluorescence images of aggregates of CdSe nanocrystals prepared on a structured LB film. (c) Average width of single fluorescence spots as a function of aggregate diameter. The intense blinking of CdSe QDs results in a broad distribution of optical spot widths for a given aggregate diameter. A line of regression reveals a strong correlation between optical width and aggregate size.

is in the range of 20–30 nm. Similar values were obtained with an imaging mode without feedback control (constant height mode), thus ruling out a topographic artifact [24]. However, a small width may also be caused by a temporal artifact based on the well-known fluorescence blinking of single CdSe nanocrystals [25]. Since this effect can equally lead to a narrowing or broadening of the real optical width, we plotted the average FWHM of every single fluorescence spot against the related aggregate diameter in order to get an average value as a measure for the true optical resolution. The resulting graph [Fig. 4(c)] shows clearly that the mean width of the fluorescence spots is strongly correlated to the size of the aggregates. Because no settling of the optical width to a constant value is observed even for the smallest aggregates, an optical resolution of clearly <40 nm can be read from the line of regression. This value is already close to the assumed lower resolution limit of half the side length of the TA, which probably is, compared to the nanosphere measurement, a result of the smaller size of the measured particles and a closer distance to the (hydrophobic) surface.

A high optical resolution can only be fully exploited, if it is accompanied by a sufficient brightness. One reason for the limitation of common aperture fiber probes is the low efficiency, by which the light is brought to the aperture [12]. Owing to its large taper angle, the TA probe with an optical resolution capability of 30–40 nm turned out to have an unusually high transmission coefficient of $\sim 10^{-4}$, which is at least 3 orders of magnitude higher than the transmission of common aperture probes of comparable resolution [12]. This opens new perspectives especially for near-field optical applications where the low brightness of conventional SNOM probes prevented so far a better optical resolution.

In conclusion, we have presented here a body of evidence showing that a triangular aperture at the tip of a tetrahedral waveguide gives rise to a new and unpredicted physical effect in near-field optics. By illuminating the aperture with light of a certain polarization, the field distribution at the aperture can be strongly confined to only one edge. Based on this effect, a new high-resolution near-field optical probe with an inherently strong suppression of background light has been developed.

We thank L. F. Chi for support and stimulating discussions, A. Rogach and H. Weller for providing the CdSe nanocrystals, and M. Bühner for taking the SEM images. This work was financially supported by the German Science Foundation (DFG, Na 382/1-1 and Na 382/1-2).

*Corresponding author.
Email address: naber@uni-muenster.de

[1] D.W. Pohl, W. Denk, and M. Lanz, Appl. Phys. Lett. **44**, 651 (1984); A. Lewis *et al.*, Ultramicroscopy **13**, 227 (1984); U. C. Fischer, J. Vac. Sci. Technol. B **3**, 386 (1985).
[2] E. Betzig *et al.*, Science **251**, 1468 (1991); E. Betzig and J. K. Trautman, Science **257**, 189 (1992).
[3] M. A. Paesler and P. Moyer, *Near-Field Optics: Theory, Instrumentation, and Applications* (John Wiley & Sons, New York, 1996).
[4] U. Ch. Fischer and D.W. Pohl, Phys. Rev. Lett. **62**, 458 (1989).
[5] L. Novotny, D.W. Pohl, and B. Hecht, Opt. Lett. **20**, 970 (1995).
[6] J. Koglin, U. C. Fischer, and H. Fuchs, Phys. Rev. B **55**, 7977 (1997).
[7] Y. Inouye and S. Kawata, Opt. Lett. **19**, 159 (1994).
[8] F. Zenhausern, Y. Martin, and H. K. Wickramasinghe, Science **269**, 1083 (1995).
[9] A. Lahrech *et al.*, Opt. Lett. **21**, 1315 (1996).
[10] B. Knoll and F. Keilmann, Nature (London) **399**, 134 (1999).
[11] E. J. Sánchez, L. Novotny, and X. S. Xie, Phys. Rev. Lett. **82**, 4014 (1999).
[12] B. Hecht *et al.*, J. Chem. Phys. **112**, 7761 (2000).
[13] J. A. Veerman *et al.*, Appl. Phys. Lett. **72**, 3115 (1998).
[14] T. Saiki and K. Matsuda, Appl. Phys. Lett. **74**, 2773 (1999).
[15] E. Betzig and R. J. Chichester, Science **262**, 1422 (1993).
[16] J. A. Veerman *et al.*, J. Microsc. **194**, 477 (1999).
[17] H. Gersen *et al.*, Phys. Rev. Lett. **85**, 5312 (2000).
[18] C. Höppener, D. Molenda, H. Fuchs, and A. Naber, Appl. Phys. Lett. **80**, 1331 (2002).
[19] A. Naber *et al.*, Rev. Sci. Instrum. **70**, 3955 (1999).
[20] H. A. Bethe, Phys. Rev. **66**, 163 (1944); C. J. Bouwkamp, Philips Res. Rep. **5**, 321 (1950).
[21] O. J. F. Martin and M. Paulus, J. Microsc. **205**, 147 (2002).
[22] A. P. Alivisatos, J. Phys. Chem. **100**, 13 226 (1996).
[23] M. Gleiche, L. F. Chi, and H. Fuchs, Nature (London) **403**, 173 (2000).
[24] B. Hecht *et al.*, J. Appl. Phys. **81**, 2492 (1997).
[25] K. T. Shimizu *et al.*, Phys. Rev. B **63**, 205316 (2001).